J Porous Mater (2016) 23:517–528
DOI 10.1007/s10934-015-0105-8

Low-temperature synthesis, structure, sorption properties and acidity of zeolite ZSM-5

Roman Barakov[1] · Nataliya Shcherban[1] · Pavel Yaremov[1] · Vladimir Solomakha[1] · Aleksey Vyshnevskyy[2] · Vladimir Ilyin[1]

Published online: 14 December 2015

Abstract High structure-directing activity and specificity of templating action of tetrapropylammonium cations TPA^+ as well as high concentration of framework-forming substances in the initial reaction mixtures contribute to the formation of zeolite ZSM-5 at relatively low temperature (100 °C) in the alkali-free media. Zeolite ZSM-5 obtained at 100 °C has higher micropore and mesopore volumes, specific surface area, less uniform micropore size distribution in comparison with ZSM-5 synthesized at 170 °C in an alkaline medium in the presence of hydrated Na^+ cations. Samples synthesized at 100 °C possess a lower concentration of acid sites and broader distribution of them in strength, compared with ZSM-5 obtained at 170 °C in an alkaline medium. ZSM-5 obtained at 100 °C exhibits a high catalytic activity in the reaction of cracking of cumene, as well as a higher selectivity to propylene and styrene, in comparison with isostructural analogue obtained at 170 °C in an alkaline medium. It is assumed that the investigated alkali-free reaction mixtures and the corresponding sol-precursors of zeolite ZSM-5 containing the elements of secondary building units can be used for obtaining of micro-mesoporous aluminosilicates in the conditions of low-temperature synthesis (100 °C) by dual-template method—in the presence of molecular and micellar templates.

✉ Roman Barakov
barakovchem07@rambler.ru

[1] L. V. Pisarzhevsky Institute of Physical Chemistry, National Academy of Sciences of Ukraine, 31 pr. Nauky, Kiev 03028, Ukraine

[2] M. P. Semenenko Institute of Geochemistry, Mineralogy and Ore Formation, National Academy of Sciences of Ukraine, 34 pr. Acad. Palladina, Kiev 03680, Ukraine

Keywords Low-temperature synthesis of ZSM-5 · Template · Alkali-free medium · The degree of crystallinity · Structure and sorption properties · Acidity · Catalytic cracking of cumene

1 Introduction

Zeolites due to its physicochemical properties, the presence of molecular sieve effect and form-selectivity effect, the high ability to a variety of chemical and structural modifications and functionalizations are widely used as adsorbents [1, 2], ion exchangers [3, 4], and catalysts in organic synthesis [5, 6], petroleum refining and petrochemicals [7, 8]. The temperature of synthesis is one of the main factors which determine the kinetics of crystallization, structure, porosity and physicochemical properties of zeolites [9]. The process of formation of zeolite in relatively mild conditions (low temperature, alkali-free medium) has a certain interest. Therefore the further study of the influence of temperature at certain values of the concentration and the ratio of reactants and pH, can afford to expand the boundaries and find out the features of zeolite formation, including the early stages of the process. The conditions close to those of individual formation of zeolites and mesoporous molecular sieves (MMS), first of all—the temperature, composition of the reaction mixture (RM), pH as well as the presence of structure-forming templates and cations of certain nature can contribute to successful direct synthesis of perspective materials—micro-mesoporous aluminosilicates (MMAS) [10, 11], combining the properties of zeolites and MMS. Taking this into account, namely—selection and providing of close conditions for the formation of zeolites and MMS, the synthesis of zeolites at relatively low temperatures in low-alkaline and/or

alkali-free media that are favorable for the formation of MMAS attracts attention.

It is known that low-silica zeolites, for example, A, X, Y, Rho types, and some others, are usually prepared at the temperatures up to 100 °C [12–17], which is caused, obviously, by the high reactivity of aluminum-enriched reaction media and its high pH values, as well as high concentration of structure-directing hydrated cations of alkali and alkaline earth metals. However, there are reports that template synthesis of some high-silica zeolites (ZSM-5, ZSM-11, β et al.) is also possible under relatively mild conditions [18]. Apparently, in these cases [19–21] namely high activity and specificity of action of the molecular template [for the formation of ZSM-5—tetrapropylammonium cation (TPA^+)] contributes to the formation of zeolites in a wide range of temperatures (70–175 °C) and pH (10.5–13.5), in the presence or absence of alkali metal cations. At the same time the process of zeolite formation at low temperatures is time-consuming and sometimes lasts up to 10 days (against from 3 to 5 days at high temperature), probably due to reducing the solubility, the rate of formation of active substances and the sites of crystallization [19]. However the prolonged induction period (up to 3 days—the synthesis of ZSM-5 at 90 °C) allows investigating the initial stages and products of crystallization more carefully [22], as well as use them as the initial building material in obtaining of MMAS.

The formation of zeolites ZSM-5 and ZSM-11 with a high degree of crystallinity is possible at 90 °C (τ = 3–5 days) in concentrated alkali and fluoride RM: H_2O/Si 3–8 for the synthesis of ZSM-5 and ~13 for ZSM-11 [18, 23]. The use of soft conditions of synthesis—hydrothermal treatment (HTT) at 70–90 °C, alkali-free reaction media—enables to restrict the growth of crystals and obtain the samples of ZSM-5 containing crystallites (10–20 nm) with a large external specific surface area (up to 200 m^2/g), strong acid sites (almost all the Al atoms are in tetrahedral positions of zeolite structure). These samples can exhibit catalytic activity in the reactions of cracking and conversion of bulk molecules, the kinetic diameter of which (>1 nm) is greater than the micropore size [24].

In accordance with this the further search and optimization of conditions of low-temperature synthesis of zeolites, comparison of their structural and sorption properties, acidity and catalytic activity with isostructural analogues obtained in conventional conditions, in particular at high temperature, seems to be actual. Accordingly, the aim of the present study is to find out the conditions and features of low-temperature synthesis of ZSM-5, as well as to carry out the comparative analysis of structural and sorption properties, acidity and activity in catalytic cracking of cumene of zeolites obtained at low (100 °C) and high (170 °C) temperature.

2 Experimental

2.1 Synthesis of the samples

Zeolite ZSM-5 (Si/Al = 50—in the initial RM) was synthesized at 100 and 175 °C in alkali-free reaction media according to the technique similar to the method described in work [25], using tetrapropylammonium hydroxide (TPAOH) as molecular template, composition of zeolite forming RM: $1.0SiO_2$: $0.01Al_2O_3$: (0.10–0.36)TPAOH: $10.83H_2O$. Aluminum nitrate nonahydrate, Aldrich, 99 % (0.078 g) and 0.9 ml of H_2O were added to the required amount of 40 % TPAOH aqueous solution, SACHEM, Inc. [1.8 ml—at TPAOH/(Si + Al) = 0.35] and the mixture was kept for 15 min at the room temperature. Then 2.3 ml of tetraethylorthosilicate (TEOS, Aldrich, 98 %) was added dropwise, stirred for 3 h (pH = 11.5–13.7) and subjected to hydrothermal treatment (HTT) at 100 °C (samples 1zt-100–5zt-100) for 3 days (sample 6zt-100 for 11 days at 100 °C); samples 7zt-170 and 8zt-170 were obtained at 170 °C similar to the previous technique (the duration of HTT for these samples was 3 days), Table 1.

For obtaining of the reference sample—zeolite ZSM-5-170 with Si/Al = 50 (Table 1) in alkali-free RM the standard technique was used, which was given in [26, 27], the composition of RM for zeolite formation: $1.0SiO_2$: $0.01Al_2O_3$: 0.19TPAOH: $17.16H_2O$. Aluminium isopropoxide [0.071 g of $Al(OiPr)_3$, Fluka, 98 %] and 4.2 ml of TPAOH, Sigma-Aldrich (20 %) were added to 3.1 ml of H_2O and the resulting mixture was stirred until dissolution of $Al(OiPrO)_3$. Then 4.8 ml of TEOS was added, stirred for 1 h and the obtained RM (pH ≈ 13.1) was subjected to HTT for 3 days at 170 °C.

For obtaining of the sample Na-ZSM-5-170 (Si/Al = 50), the RM of which contains Na^+, the typical RM for forming this zeolite was used: $1.0SiO_2$: $0.012Al_2O_3$: 0.38TPAOH: 0.024NaOH: 0.61NaCl: $178H_2O$, similar to that was used in the work [28] (Table 1). As-synthesized aluminum hydroxide (0.14 g) containing 10 wt% of Al_2O_3, sodium chloride (0.41 g), 4.2 ml of TPAOH solution (22 %) and NaOH (0.01 g) were sequentially added to 33 ml of water and the obtained mixture was stirred until complete dissolution of aluminum hydroxide. Than 2.6 ml of TEOS was added, the mixture was stirred for another 2 h (pH ≈ 11) and subjected to HTT at 170 °C for 2 days.

All obtained samples (initial, intermediate and final products of the synthesis) were prepared for further investigation and characterization by standard technique: washed with distilled water, dried and calcined in air at 550 °C for 5 h (heating rate 2 °C/min). The reference sample of zeolite (in Na-form) after calcination was subjected to ion exchange in 1 M NH_4Cl solution at 40 °C for

Table 1 The synthesis conditions and the degree of crystallinity of zeolites samples

Samples	TPAOH/(Si + Al)	HTT of the reaction mixture of zeolite		pH of the reaction mixture of zeolite		The degree of crystallinity
		T (°C)	τ[a] (days)	Before HTT	After HTT	
1zt-100	0.10	100	3	11.2	11.2	Amorphous
2zt-100	0.14	100	3	11.5	13.1	0.90
3zt-100	0.18	100	3	12.3	13.6	1
4zt-100	0.27	100	3	13.3	13.8	0.15
5zt-100	0.35	100	3	13.7	13.7	0.15
6zt-100	0.35	100	11	13.4	13.9	0.10
7zt-170	0.14	170	3	11.5	13.2	0.70
8zt-170	0.35	170	3	13.7	13.7	0.50
ZSM-5-170	0.19	170	3	13.1	11.9	0.80
Na-ZSM-5-170	0.37	170	2	11.0	11.9	0.80

[a] Duration of HTT

24 h for obtaining of NH_4^+-form and then converted to H-form (H-ZSM-5-170) by standard procedure (heating to 550 °C with rate 2 °C/min, holding time 5 h).

2.2 Characterization of samples

Phase composition of the obtained samples was analyzed using X-ray diffractometer D8 ADVANCE (Bruker AXS) with CuK_α-radiation. The degree of crystallinity was evaluated by change in the ratio of the intensities of the characteristic reflections at $2\theta = 23.0°$; 23.8°; 24.2° of the investigated samples and sample 3zt-100 with the most intense reflections in the XRD pattern, for which the degree of crystallinity was adopted as one. The crystallite size of ZSM-5 was calculated by the Scherrer's equation [29].

The method of dynamic light scattering (DLS)—Malvern Instruments' Zetasizer Nano S, was used to estimate the particle size of sol-precursors in RM for zeolite formation as well as particle size of the obtained zeolite samples (before the measurement the sample was dispersed in water in an ultrasonic bath within 15 min, the concentration of suspension was 0.1 wt%); measurement accuracy was ±2 %.

IR spectra of the initial and calcined samples (tablets with KBr, 1: 100) were recorded on the Fourier spectrometer Spectrum One (Perkin Elmer).

The SEM images were obtained by using field emission SEM JSM-6700 F («JEOL»). Images were generated using an accelerating voltage of 15 kV and a beam current of 0.65 nA. Before imaging samples were coated, using sputtering method, by platinum film of 15 nm thickness.

The chemical composition of samples was determined using a SEM JSM-6700F equipped with a JED-2300 energy-dispersive spectrometer («JEOL»). Operating conditions were as follows: 15 kV accelerating voltage, 0.65 nA beam current, 2 μm beam size and a counting time of 60 s for one analysis. Pure Al and Si were used for calibration. Raw counts were corrected for matrix effects with the ZAF algorithm implemented by «JEOL».

Nitrogen adsorption was measured by volumetric method (77 K, up to 1 atm) on the analyzer of porous materials Sorptomatic 1990 (Thermo Electron Corp.). Samples were previously evacuated ($p \sim 0.7$ Pa) at 350 °C for 5 h. The total specific surface area S_{BET} was evaluated according to [30]; the micropore size was calculated by the method of Saito and Foley [31]; the mesopore size distribution was determined on the adsorption branch, in accordance with [32, 33], and desorption branch of the isotherm, using the method of Barret et al. [34]; the mesopore volume as well as mesopore specific surface area and external surface area were determined by the comparative *t-plot* method [35]. The characteristic energy of adsorption E_0 and micropore volume were determined by the Dubinin–Radushkevich equation of the theory of volume filling of micropores [36].

The acidic properties of the samples were investigated by the standard method of temperature-programmed desorption of ammonia (TPDA) [37]: the sample was activated for 30 min in a flow of helium at 550 °C (heating rate to a given temperature was 15 °C/min), cooled to 100 °C and saturated with ammonia for 20 min; physically bound NH_3 was desorbed by venting with helium at 100 °C; the remaining NH_3 was desorbed by heating in the temperature range 100–700 °C (15 °C/min); the position of the maximum of desorption was determined using chromatograph (thermal conductivity detector) and recorded as curve of TPDA and the amount of desorbed ammonia was determined by titrating with 1×10^{-3} M solution of

hydrochloric acid. The peaks of thermal desorption of NH_3 were determined by deconvolution of TPDA curves by using the Gaussian distribution.

The method of ad(de)sorption of pyridine with IR-spectral control generally acceptable in the study of zeolites was used for characterization of the nature, strength and quantity of acid sites [38]. The thin plates of the studied samples (8–12 mg/cm^2, without binder) were placed in a cuvet with NaCl windows and evacuated (p = 1.4 Pa) at 400 °C for 1 h; pyridine was adsorbed at 150 °C for 15 min, and desorbed at 150–400 °C (step 50 °C, holding time 30 min). The concentration of Lewis (L-sites) and Brønsted (B-sites) acid sites was determined by integral intensity of the absorption bands at 1454 and 1545 cm^{-1} respectively with using of the integral molar extinction coefficients for these bands: ε(L) = 2.22 cm/μmol and ε(B) = 1.67 cm/μmol [39].

For determining the nature, strength and concentration of acid sites located on the external surface of the samples the method of ad(de)sorption of 2,6-di-*tert*-butylpyridine with IR-spectral control was used [40]. The technique of the experiment is similar to the methods described above for the ad(de)sorption of pyridine. The concentration of B-sites was determined by integral intensity of the absorption band at 1530 cm^{-1} with using of the integral molar extinction coefficient for this band: ε(B) = 1.67 cm/μmol [41].

The catalytic cracking of cumene on the obtained samples was performed in the micropulsed mode (carrier gas—helium, flow rate—15 cm^3/min) at atmospheric pressure in the temperature range 300–400 °C (step 25 °C). The samples were previously activated for 1 h in a flow of helium (10 cm^3/min) at 550 °C. For the analysis of the cracking products the gas chromatograph «Cvet-104» was used with a flame ionization detector and a packed column with an internal diameter of 3 mm and a length of 2 m. The packed column was filled with solid phase «Inerton AW-10-dimethyldichlorosilane» (fraction 0.2–0.25 mm), on which the active phase XE-60 in amount of 5 wt% was deposited. The conversion of cumene (X) was calculated as the sum of yield of the reaction products in mol%. The selectivity towards each of the reaction products (in mol%) was calculated from the formula S = (Y/X)·100, where Y—product yield (in mol%).

3 Results and discussion

Zeolite is not formed in the conditions of HTT at 100 °C for 3 days and under ratio of TPAOH/(Si + Al) = 0.10 in zeolite forming RM of ZSM-5 on the basis of aluminum nitrate and TEOS (Si/Al = 50—in the initial RM)—the sample 1zt-100 is X-ray amorphous (Fig. 1; Table 1).

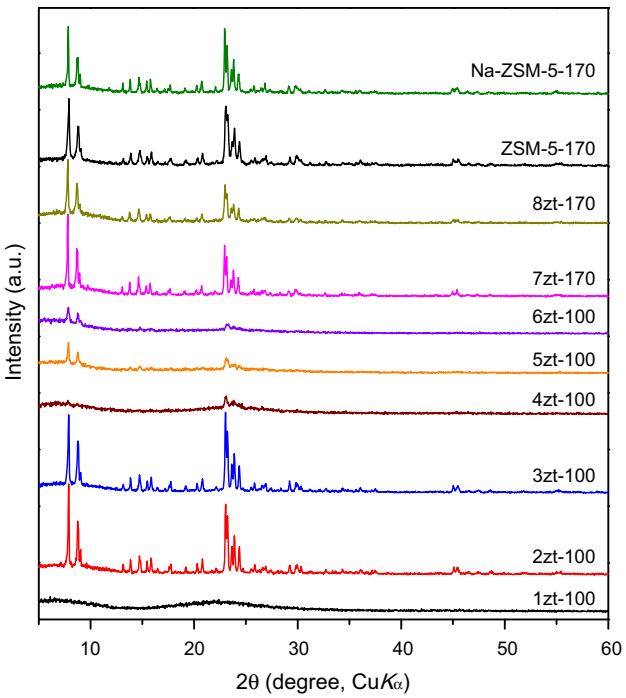

Fig. 1 XRD patterns of the samples 1zt-100–6zt-100, 7zt-170, 8zt-170, ZSM-5-170, Na-ZSM-5-170 (the synthesis conditions are presented in Table 1)

Probably due to the fact that the dissolution of the hydrolysis products of TEOS is complicated at pH ~ 11 and the corresponding concentration of OH^- ions. With increasing the ratio of TPAOH/(Si + Al) up to 0.14 (pH = 11.5) and 0.18 (pH = 12.3) respectively the crystallization of ZSM-5 is possible already (samples 2zt-100 and 3zt-100). These samples (2zt-100 and 3zt-100) with particle size ~0.6 and ~0.4 μm (by the DLS) respectively possess zeolite structure with high degree of crystallinity. This is evidenced by the high intensity of the characteristic reflections in the XRD pattern, their good resolution and display of fine structure of diffraction lines (Fig. 1), as well as the presence of absorption band at ~550 cm^{-1}, which can be attributed to the asymmetric stretching vibrations of (alumino)siloxane bonds in the five-membered rings of $Si(Al)O_{4/2}$ tetrahedra [42, 43] in IR spectra of these samples (Fig. 2). The intensity of this band is close to that of the samples of ZSM-5-170 and Na-ZSM-5-170 with high degree of crystallinity (Table 1), that are obtained at elevated temperatures in alkali-free and alkaline medium respectively. Noticeable increase in pH of zeolite forming RM after HTT (to 13.1 for 2zt-100 and 13.6 for 3zt-100) can be associated with the inclusion of silicate ions in zeolite structure and, consequently, an increase in the ratio of concentrations $[OH^-]/[SiO_2]$ in the solution [22].

With further increase in the ratio TPAOH/(Si + Al) up to 0.27 and 0.35 (pH = 13.3 and 13.7 respectively) in

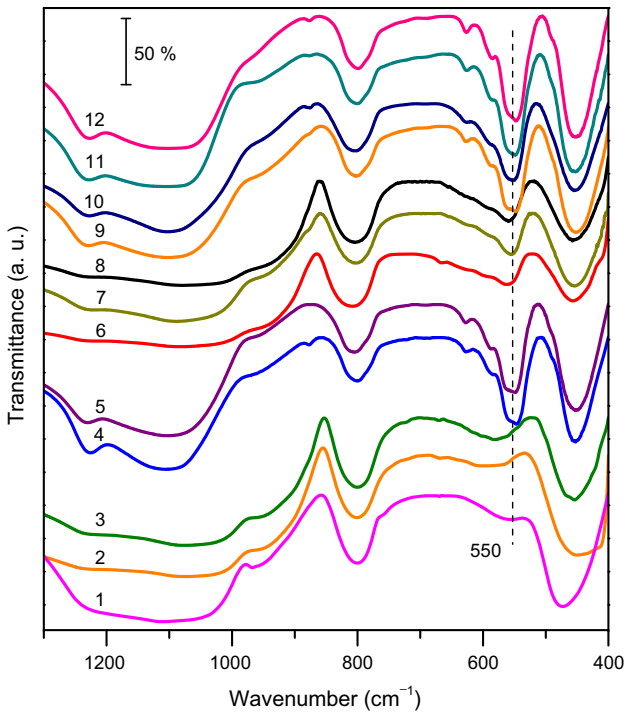

Fig. 2 FTIR spectra of the dispersed phase of the initial zeolite forming RM, TPAOH/(Si + Al) = 0.35 (*1*), sol-precursor after preliminary HTT of the RM of zeolite at 100 °C for 1 day (*2*), sol-precursor after preliminary HTT of the RM of zeolite at 100 °C for 2 day (*3*), samples 2zt-100 (*4*)–6zt-100 (*8*), 7zt-170 (*9*), 8zt-170 (*10*), ZSM-5-170 (*11*), Na-ZSM-5-170 (*12*)

initial zeolite forming RM at the same conditions (100 °C, 3 days), the degree of crystallinity of the samples 4zt-100 and 5zt-100 (Fig. 1; Table 1) is significantly reduced (up to 0.15). Besides, the intensity of characteristic band at 550 cm^{-1} in IR spectra of these samples is decreased, which is probably due to the increase of solubility of aluminosilicate. It should be noted that the initial zeolite forming RM [TPAOH/(Si + Al) = 0.35], containing X-ray amorphous particles with size from 1.1 to 4.2 nm (maximum on distribution curve ~2 nm, which corresponds to the data of work [44]) and X-ray amorphous sol-precursors, that were obtained by preliminary HTT of the RM of zeolite at 100 °C for 1 day (particle size 21–43 nm, average size—28 nm) and 2 days (particle size of 18–90 nm, average size—40 nm) contain the elements of secondary building units of ZSM-5 (Fig. 2). Increasing of the duration of HTT of RM of zeolite [TPAOH/(Si + Al) = 0.35] up to 11 days does not lead to an increase in crystallinity (Fig. 1; Table 1), as well as intensity of absorption band at 550 cm^{-1}—sample 6zt-100 (Fig. 2). The samples 4zt-100, 5zt-100 and 6zt-100 contain mainly amorphous particles with size 0.3–0.4 μm; the crystallites of ZSM-5 with size 80–110 nm (estimated by Scherrer equation) are also presented in these samples.

Increasing of the temperature of HTT of RM of zeolite [TPAOH/(Si + Al) = 0.14, pH = 11.5] to 170 °C (sample 7zt-170, Table 1) results to some decrease of the degree of crystallinity (up to 0.7) compared with samples 2zt-100 and 3zt-100, that can be caused by increase in solubility of aluminosilicate with increasing the temperature of synthesis. Besides, the sample 7zt-170, along with predominantly large particles with size ~1 μm (by the DLS), contains the particles with size ~0.25 μm. The increase of the degree of crystallinity, at ratio TPAOH/(Si + Al) = 0.35, up to 0.5, in comparison with sample 6zt-100, is possible with increasing of the temperature of HTT up to 170 °C (sample 8-zt-170, Fig. 1; Table 1); wherein, the particle size reaches 0,45 μm and the intensity of absorption band at ~550 cm^{-1} in the IR spectrum of this sample is almost the same as for the fully crystalline sample 3zt-100 (Fig. 2).

It is obvious that the decrease in temperature of synthesis leads to increase of the induction period and slowing of crystallization (decrease in the rate of crystallization) [45]; which is consistent with experimental data—the nucleation process at 100 °C begins after 35 h of HTT (sample 3zt-100), in high-temperature synthesis (160 °C)—after 27 h (sample ZSM-5-160); the degree of crystallinity of the samples 3zt-100 and ZSM-5-170 after 48 h of HTT is 0.2 and 0.4 respectively. The degree of crystallinity of the sample Na-ZSM-5-170 is ~0.8 after HTT of RM containing Na^+ cations, for 3 h (at 170 °C), which is probably due to their high structure-forming activity in these conditions of synthesis [46].

According to SEM data the sample 2zt-100 (Fig. 3a) consists of crystallites of spherical shape with size from 0.4 to 0.7 μm (maximum of distribution is ~0.55 μm, Fig. 3d). The shape of these crystallites is more pronounced than that of the sample ZSM-5-170 (Fig. 3b, maximum of distribution is ~0.45 μm, Fig. 3e), which was synthesized at 170 °C in the alkali-free RM. Sample 7zt-170 contains larger particles (maximum of distribution is ~0.9 μm, Fig. 3f), which probably consist of small crystallites with size up to 100 nm (Fig. 3c). In this sample the small proportion of crystals with size of about 2.5 μm is also presented. Their occurrence is associated with an increase in temperature of HTT from 100 (sample 2zt-100) to 170 °C (sample 7zt-170). The particles of the samples 2zt-100, ZSM-5-170 and 7zt-170 have the less defined shape and smaller size in comparison with zeolite ZSM-5 (crystal size with shape of prisms is ~4–5 μm), obtained in conventional conditions at 170 °C in an alkaline medium [28, 47]. This can be due to the absence of hydrated Na^+ cations in the used RM (as in the RM of the samples 2zt-100, 7zt-170 and ZSM-5-170). The Na^+ cations exhibit the high structure-forming activity and contribute to the

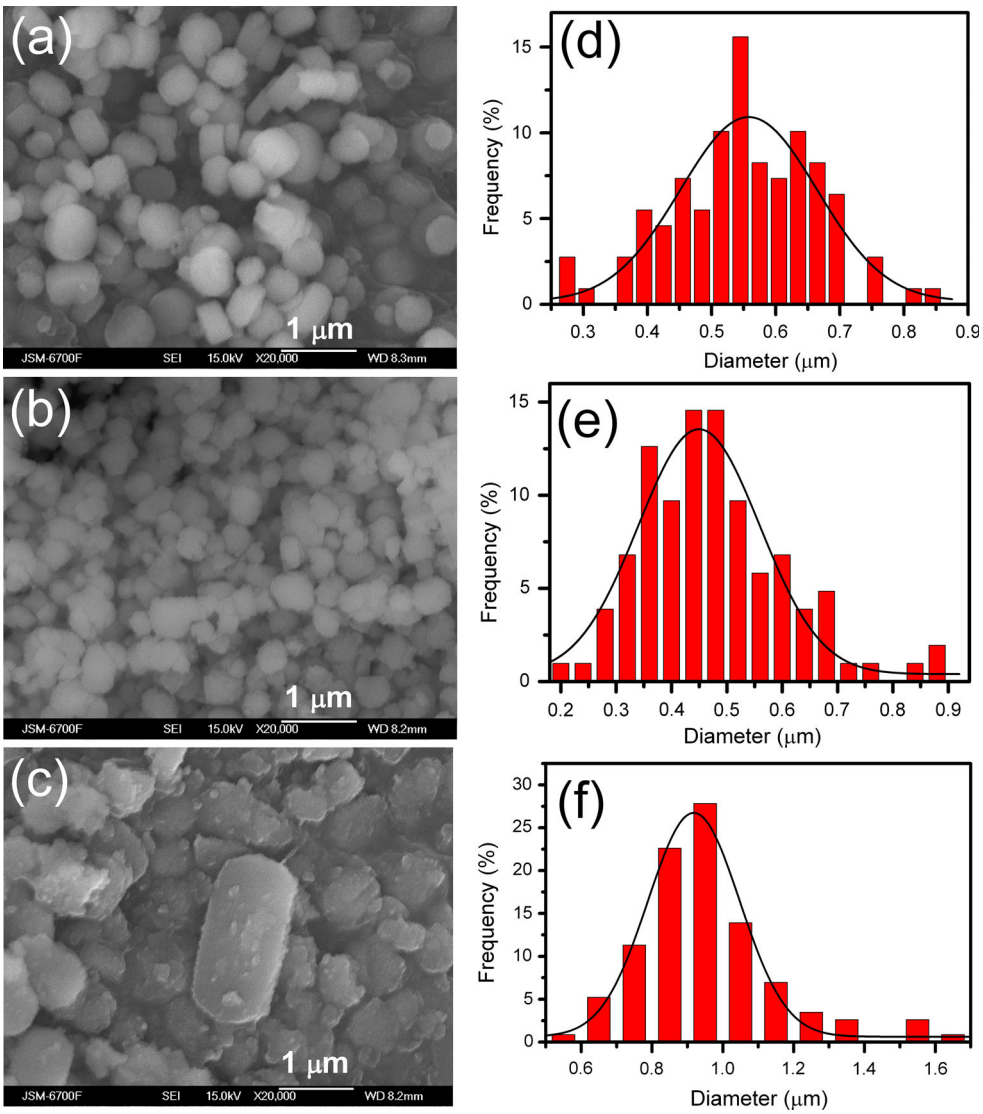

Fig. 3 SEM images (**a**–**c**) and particle size distribution (**d**–**f**, according to SEM) of the samples 2zt-100 (**a**, **d**), ZSM-5-170 (**b**, **e**), 7zt-170 (**c**, **f**)

formation of large, uniform crystals with well-defined edges and faces.

Structural and sorption characteristics of sample 2zt-100 in general are similar to zeolite ZSM-5 (Fig. 4; Table 2) and do not differ substantially from ZSM-5-5-170, which was obtained at 170 °C in alkali-free reaction medium with similar composition. Sample 2zt-100 possesses higher S_{BET} (470 m^2/g) compared to ZSM-5-170 (S_{BET} = 425 m^2/g).

Increasing of the temperature of HTT of alkali-free RM (100 °C → 170 °C) leads to obtaining of the sample 7zt-170, which possesses mesopores: volume V_{meso} = 0.19 cm^3/g, diameter D_{meso} = 7.2 nm (by the adsorption branch of the isotherm), 6.3 nm (by the desorption branch), surface area S_{meso} = 160 m^2/g and has higher total pore volume (V_t = 0.35 cm^3/g) and external surface area (S_{ext} = 70 m^2/g) in comparison with samples 2zt-100, ZSM-5-170 and Na-ZSM-5-170 (Table 2). Formation of mesopores (Fig. 4c) in the sample 7zt-100 can be associated with a reduction in crystallites size due to an increase of solubility of silica at higher temperatures [24] and generation of the secondary structure from the aggregates of condensed nanoparticle.

Increasing of the ratio TPAOH/(Si + Al) from 0.14 to 0.35 (samples 7zt-170 and 8zt-170 respectively) leads to an increase in external surface area (70 → 135 m^2/g). This is probably because the TPA^+ cations at high concentrations [TPA^+/(Si + Al) = 0.35] can compensate the negative charge on the external surface of particles, prevent their aggregation and thus slow down the growth of crystals and promote the formation of crystallites with size ~0.45 μm (by the DLS)—sample 8zt-175, which is consistent with the data of [16, 48].

There are significant differences under comparing the characteristics of the porous structure of the sample 2zt-

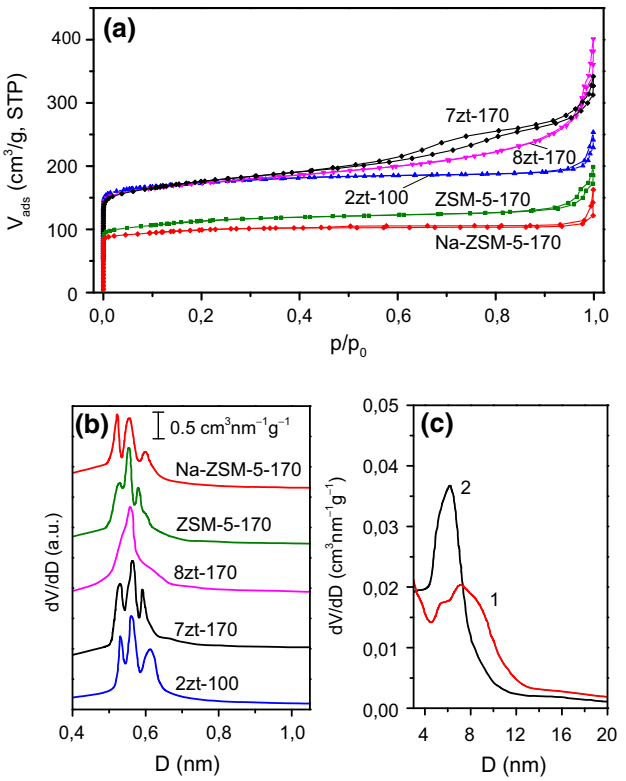

Fig. 4 Nitrogen ad(de)sorption isotherms at 77 K (**a**) and micropore size distribution (**b**) for samples 2zt-100, 7zt-170, 8zt-170, ZSM-5-160 and Na-ZSM-5-170 (the isotherms of the samples 2zt-100, 7zt-170, 8zt-170 are vertically offset by 50 cm^3/g), mesopore size distribution (**c**) for sample 7zt-170 calculated from the adsorption (*1*) and desorption (*2*) branches of the isotherm

100 with zeolite Na-ZSM-5-170 obtained at 170 °C in alkaline medium, as it could be expected. Sample 2zt-100 has larger micropore volume ($V_{micro} = 0.17$ cm^3/g), V_t (0.22 cm^3/g), S_{BET} (470 m^2/g) compared to Na-ZSM-5-170 (Table 2). The reason of this is a high structure-forming activity of the hydrated Na^+ cations along with that one of the organic template—TPA^+ [9, 46]. Herewith the characteristic energy of adsorption E_0 for sample 2zt-100 (5.1 kJ/mol) is smaller than for samples ZSM-5-170 (5.7 kJ/mol) and Na-ZSM-5-170 (6.1 kJ/mol, Table 2) probably due to the fact that the sample 2zt-100 has larger micropores (Fig. 4b). The differences in E_0 can also be caused by different types of adsorption sites (including the silanol groups and acid sites of different nature and strength) and their location on the external surface or in the micropores of these samples.

The calcined sample 2zt-100 (Si/Al in the sample—27) has slightly stronger acid sites—maximum of thermal desorption of ammonia is at 435 °C (concentration is 120 μmol/g), Fig. 5, in comparison with the sample 8zt-170 (Si/Al—24)—maximum of thermal desorption is at 410 °C (concentration is 150 μmol/g). It can be assumed, in accordance with [49], that the sample 8zt-170 possessing larger external surface area (S_{ext}—135 m^2/g, against 15 m^2/g in 2zt-100) contains larger amount of strong acid sites on external surface, from which the ammonia desorbs at a lower temperature than from micropores (due to higher adsorption potential and diffusional difficulties of desorption of ammonia). The maximum of desorption at 200–210 °C is apparently due to interaction of ammonia with surface silanol groups resulting in the formation of hydrogen bond (weakly bounded NH_3). In comparison with decationized sample of H-ZSM-5-170 (by preliminary ion-exchange of Na^+ on NH_4^+ and subsequent heating at 550 °C), that was obtained on the basis of the sample Na-ZSM-5-170 (Fig. 5), the sample 2zt-100 has a lower concentration of acid sites (120 μmol/g, in H-ZSM-5-170—136 μmol/g) and a broader distribution of these sites by

Table 2 Structural and sorption characteristics of the samples determined by N_2 ad(de)sorption, 77 K

Samples	Microspores		Mesopores			V_t (cm^3/g)	S_{BET} (m^2/g)	S_{ext} (m^2/g)	E_0 (kJ/mol)
	V_{micro} (cm^3/g)	D_{micro} (nm)	V_{meso} (cm^3/g)	D_{meso} (nm)	S_{meso} (m^2/g)				
2zt-100	0.17	0.56	0.05	–	135	0.22	470	15	5.1
7zt-170	0.16	0.56	0.19	7.2[a]; 6.3[b]	160	0.35	455	70	4.6
8zt-170	0.17	0.55	0.17	–	115	0.34	455	135	4.8
ZSM-5-170	0.16	0.55	0.05	–	140	0.21	425	20	5.7
Na-ZSM-5-170	0.14	0.55	0.02	–	95	0.16	375	5	6.1

V_{micro}, micropore volume; D_{micro}, average micropore diameter; V_{meso}, mesopore volume; D_{meso}, mesopore diameter; S_{meso}, mesopore specific surface area; V_t, total pore volume at $p/p_0 = 0.95$; S_{BET}, total specific surface area; S_{ext}, external surface area; E_0, characteristic energy of adsorption

[a] Mesopore diameter calculated from the adsorption branch of the isotherm

[b] Mesopore diameter calculated from the desorption branch of the isotherm

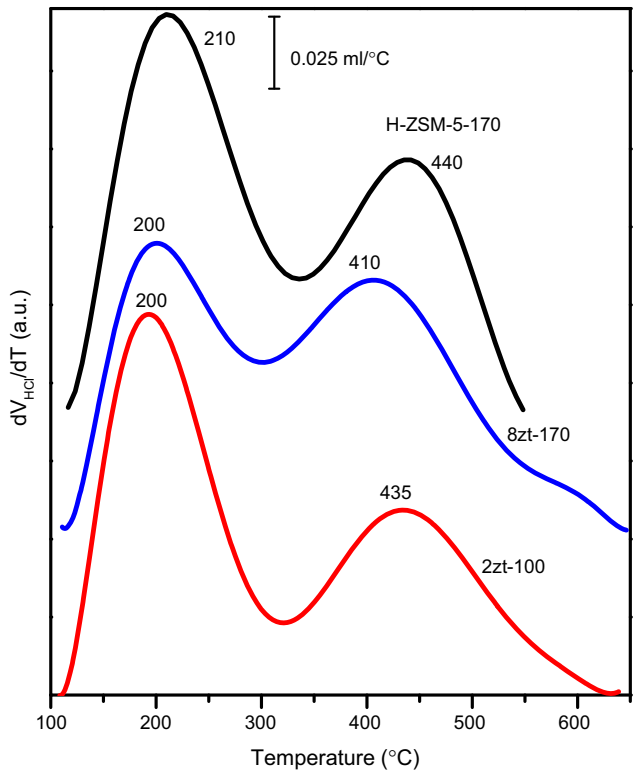

Fig. 5 NH_3-TPD profiles for samples 2zt-100, 8zt-170 and H-ZSM-5-170

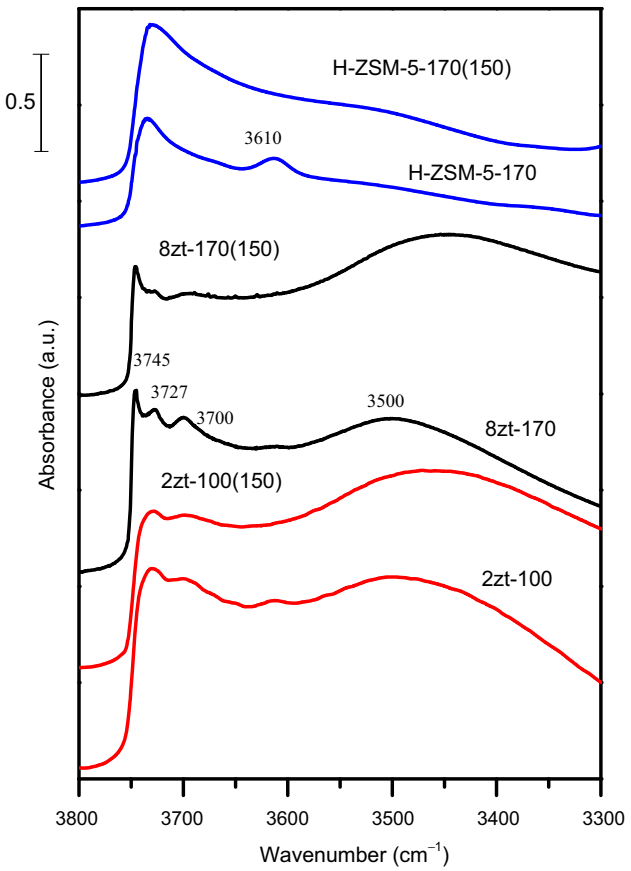

Fig. 6 FTIR spectra of samples 2zt-100, 8zt-170 and H-ZSM-5-170 (in the region of vibrations of OH-groups) after preliminary evacuation at 400 °C and after adsorption of pyridine and its desorption at 150 °C: 2zt-100(150), 8zt-170(150), H-ZSM-5-170(150)

strength (Fig. 5). It can be due to the presence (in sample 2zt-100) of Lewis acid sites as well as OH-groups (on which the ammonia can be adsorbed) bonded with the aluminum atoms, which located in an octahedral coordination, in addition to Brønsted acid sites, that typical for zeolites. The extra-framework aluminum species and structural defects (three-coordinated Al atoms) [50] can be attributed to the Lewis acid sites. These differences can also be caused by the change of bond lengths and angles of Si–OH–Al in the sample 2zt-100 in comparison with the H-ZSM-5-170.

In IR spectra of the samples 2zt-100, 8zt-170 and H-ZSM-5-170 after evacuation at 400 °C the absorption band is observed in the range of 3727–3735 cm^{-1} (Fig. 6). This band corresponds to the stretching vibrations of O–H in silanol groups, the presence of which is associated with incomplete condensation of the framework [51]. In the spectrum of the sample 8zt-170, which possesses higher S_{ext} (135 m^2/g) compared to 2zt-100 and H-ZSM-5-170 (Table 2), the absorption band (Fig. 6) is also presented at 3745 cm^{-1}, which can be attributed to the vibrations of O–H bond of silanol groups located on the external surface of the sample [51]. In the spectra of samples 2zt-100 and 8-zt-100, in contrast to the H-ZSM-5-170, the absorption bands are observed at 3700 cm^{-1} and about 3500 cm^{-1}, which corresponds to the vibrations of O–H in hydroxyl groups bounded with aluminum atoms in octahedral coordination [52] and the vibrations of O–H in H-bonded silanol groups [51]. Consequently, zeolite ZSM-5 obtained at 100 °C, contains more defects in the structure (e.g., silanol groups or T-vacancies, due to the lack of framework-forming atoms in the lattice sites) compared with H-ZSM-5-170—decationized form of Na-ZSM-5-170 obtained at high temperature [53]. The presence of absorption band at 3700 cm^{-1} in the spectra of samples 2zt-100 and 8zt-100 can indicate that these samples have extra-framework aluminum species [51], the formation of which can be caused by lack of Na^+ cations in RM. These cations facilitate the inclusion of aluminium into the framework and its stabilization in the tetrahedral oxygen surrounding (this absorption band is not present in the spectrum of H-ZSM-5-170, Fig. 6). In the spectra of the samples 2zt-100 and ZSM-5-170 the absorption band at 3610 cm^{-1} is also presented (Fig. 6, it is weak in the spectrum of 8zt-170), which corresponds to the stretching vibrations of O–H in the bridging hydroxyl groups Si–OH–Al (B-sites) [51]. As a result of pyridine interaction with B-sites the

absorption band at 3610 cm^{-1} disappears, at the same time, in the IR spectra of the all samples recorded after desorption of pyridine at 150–400 °C (Fig. 7, 8, 9), the absorption bands at 1548 and 1456 cm^{-1} are appeared, corresponding to the stretching vibrations of bonds of pyridine ring adsorbed on the bridging OH-groups (B-sites) as a pyridinium ion PyH^+, as well as pyridine molecules interacting with the coordinatively-unsaturated aluminum ions (L-sites), respectively (Fig. 7, 8, 9) [51]. At the same time the intensity of the absorption band at 3700 cm^{-1} is decreased in IR spectra of samples 2zt-100 and 8zt-170 (Fig. 6), that can be due to the interaction of pyridine with Al–OH-groups (aluminium atoms are in octahedral coordination) with formation of hydrogen bond (pyridine is completely desorbed from these groups at 250 °C). The sample H-ZSM-5-170 mainly possesses the strong B-sites (the concentration is 113 μmol/g), the absorption bands at 1548 and 1639 cm^{-1} remain in the IR spectrum after desorption at 400 °C (Fig. 9). The samples 2zt-100 and 8zt-170 in addition to B-sites (the concentration is 40 and 50 μmol/g

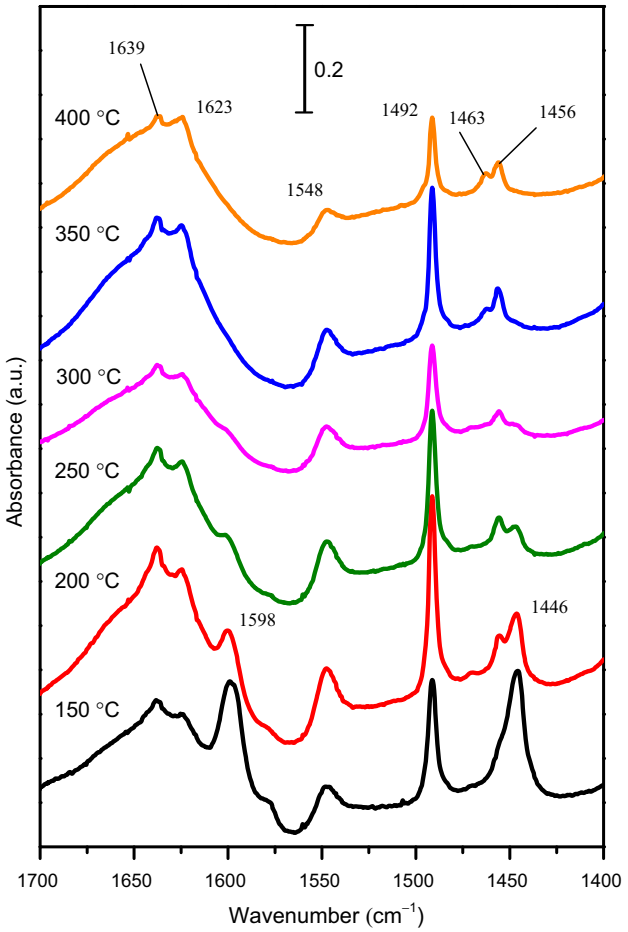

Fig. 7 FTIR spectra of sample 2zt-100 in the region of 1700–1400 cm^{-1} recorded after adsorption of pyridine at 150 °C and its desorption at 150–400 °C

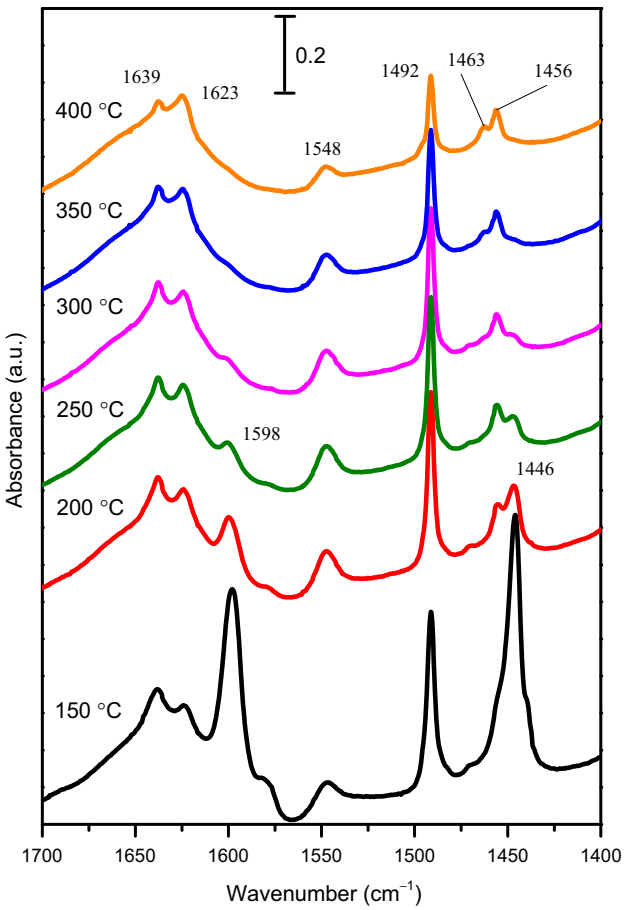

Fig. 8 FTIR spectra of sample 8zt-170 in the region of 1700–1400 cm^{-1} recorded after adsorption of pyridine at 150 °C and its desorption at 150–400 °C

respectively, the pyridine remains after evacuation at 400 °C), also contain L-sites (the absorption bands at 1456, 1463 and 1623 cm^{-1}, the concentration is ~40 μmol/g, the absorption bands remain after evacuation at 400 °C) and silanol groups (the absorption bands at 1446 and 1598 cm^{-1}) interacting with pyridine (the absorption bands do not appear after evacuation at 350 °C, Fig. 7, 8).

The investigation of ad(de)sorption of 2,6-di-*tert*-butylpyridine (DTBPy) allowed to characterize the nature, concentration and strength of acid sites located only on the external surface of the samples of zeolites, since the micropores of zeolite ZSM-5 are not accessible for the molecules of DTBPy (the kinetic diameter of DTBPy is 0.8 nm) [38]. In IR spectra of the samples 2zt-100, 8zt-170 and H-ZSM-5-170 (Fig. 10) recorded after adsorption of DTBPy (at the temperature of 150 °C) and its desorption at the same temperature, the absorption bands at 1615 and 1530 cm^{-1}, corresponding to the stretching vibration of bonds of DTBPy ring adsorbed on the bridging OH-groups in the form of $DTBPyH^+$ ion [41] are presented. The sample 8zt-170 with the external surface of 135 m^2/g

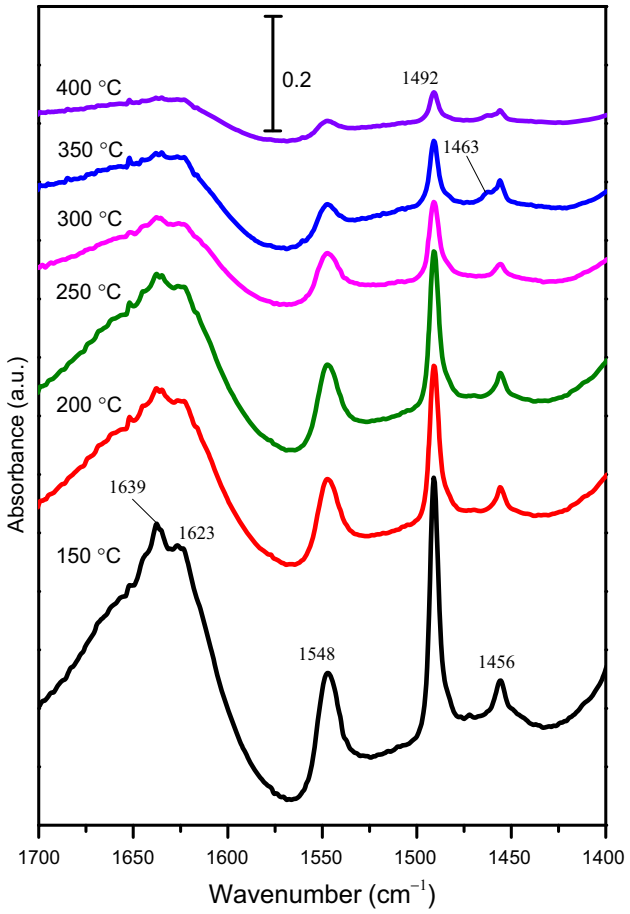

Fig. 9 FTIR spectra of sample H-ZSM-5-170 in the region of 1700–1400 cm^{-1} recorded after adsorption of pyridine at 150 °C and its desorption at 150–400 °C

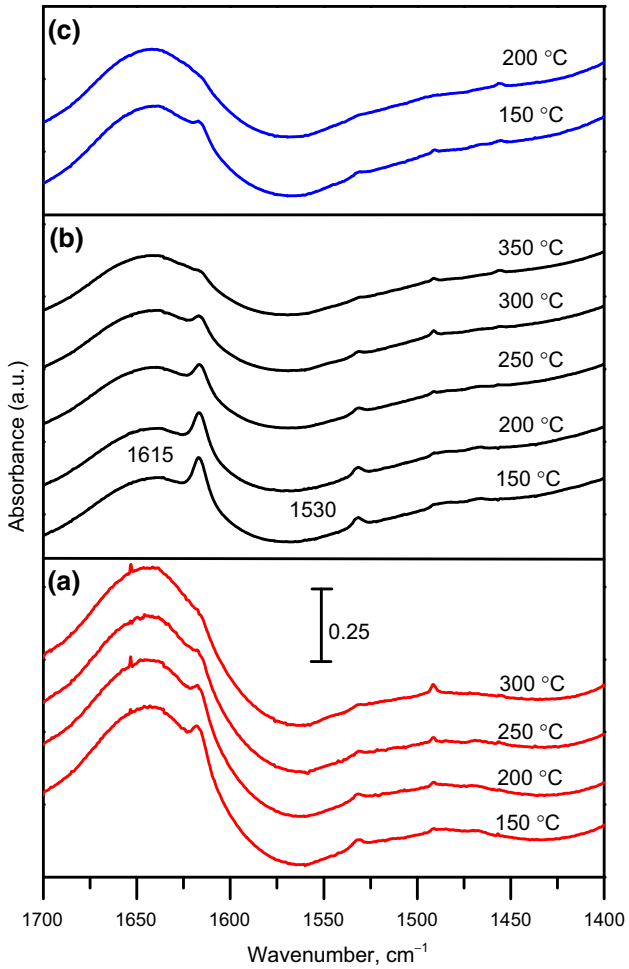

Fig. 10 FTIR spectra of the samples 2zt-100 (**a**), 8zt-170 (**b**), H-ZSM-5-170 (**c**) in the region of 1700–1400 cm^{-1} recorded after adsorption of 2,6-di-*tert*-butylpyridine and its desorption at different temperatures

(Table 2) possesses the higher concentration of Brønsted acid sites, which are accessible for DTBPy (11 μmol/g, temperature of the complete desorption is 350 °C), compared with 2zt-100 (4 μmol/g, pyridine is completely desorbed at 300 °C) and H-ZSM-5-170 (3 μmol/g, pyridine is completely desorbed at 200 °C), the external surface of which is negligible (15 m^2/g—2zt-100, 5 m^2/g—H-ZSM-5-170).

The results of previous [16, 18, 24] and the present studies indicate that the processes of dissolution-reprecipitation of the initial substances with formation of active dissolved compounds and precursors, the generation of nucleation sites and the process of the crystallization of ZSM-5 as a whole are possible in the used conditions—at relatively low temperatures and in alkali-free media. The apparent activation energy (E_a) of formation of zeolite ZSM-5 is in the range of 40–90 kJ/mol (at a temperature range of 80–175 °C) according to [54, 55]. These values of E_a indicate, in accordance with [46, 54], that the interaction between the active dissolved substances with formation of zeolite precursors, as well as between the primary particles—building units with formation of nuclei or condensation of the dissolved compounds on the growing crystal faces, rather than the process of diffusion of dissolved compounds to the surface of nuclei or crystals, for which the E_a is significantly smaller—approximately 12–17 kJ/mol [46] can be the limiting stage of the formation of zeolite ZSM-5. The possibility of zeolite formation in the used RM at 100 °C (though, obviously, with smaller/slower rate of nucleation and crystal growth [46, 56]) can be attributed to the high structure-directing activity and specificity of action of TPA^+ cations toward the formation of zeolite ZSM-5 (as probably and cations—TEA^+, TBA^+) in alkali-free RM, as well as high concentration of reactants in the initial RM: $H_2O/(SiO_2 + Al_2O_3) = 11$, in most of the experiments on the synthesis at 160–170 °C—$H_2O/(SiO_2 + Al_2O_3) = 30$–180 [26, 28, 57], which is consistent with the data of [18, 24, 58].

Table 3 The catalytic conversion of cumene on the synthesized samples, products selectivity and propylene/benzene molar ratio at different temperatures of the process

Samples	T (°C)	Conversion of cumene (mol%)	Selectivity (mol%)					Propylene/benzene molar ratio
			Propylene	Benzene	Toluene	Ethylbenzene	Styrene	
2zt-100	300	96.7	42.2	52.5	1.5	1.6	2.2	0.80
	325	97.2	44.3	49.7	1.5	1.9	2.6	0.89
	350	98.0	43.0	51.3	1.6	2.0	2.1	0.84
	375	98.5	40.1	54.2	1.7	2.3	1.7	0.74
	400	98.9	42.9	51.2	1.9	2.7	1.3	0.84
H-ZSM-5-170	300	98.1	37.9	55.6	3.1	1.9	1.5	0.68
	325	98.7	37.5	54.4	3.8	2.9	1.4	0.69
	350	98.9	38.3	53.5	3.7	3.3	1.2	0.72
	375	99.1	40.9	50.9	3.6	3.6	1.0	0.80
	400	99.2	41.0	50.2	4.0	3.9	0.8	0.82

Samples 2zt-100 and H-ZSM-5-170 were tested in a model reaction of catalytic cracking of cumene [59]. Sample 2zt-100 obtained at 100 °C exhibits a high catalytic activity in the entire investigated range of temperatures (300–400 °C, the conversion of cumene is 96.7–98.9 mol%), which is comparable with the decationized form of Na-ZSM-5-170 obtained at 170 °C in an alkaline medium—sample H-ZSM-5-170 (98.1–99.2 mol%). Both samples exhibit a high selectivity to the major products of the cracking reaction—propylene (40.1–44.3 mol% for 2zt-100, 37.5–41.0 mol% for H-ZSM-5-170) and benzene (49.7–54.2 mol% for 2zt-100, 50.2–55.6 mol% for H-ZSM-5-170), Table 3. The propylene/benzene molar ratio (0.74–0.89) is higher for the sample 2zt-100, in comparison with H-ZSM-5-170 (0.68–0.82), Table 3. This can indicate that a more active propylene oligomerization occurs on the sample H-ZSM-5-170 with a higher concentration of Brønsted acid sites. The products of propylene oligomerization remain on the sample in the form of coke precursors. The selectivity to toluene and ethylbenzene (byproducts) is higher for the sample H-ZSM-5-170 compared with 2zt-100 (Table 3), that can also be associated with a higher concentration of strong Brønsted acid sites in ZSM-5 obtained at 170 °C. Ethylbenzene can also be formed on the Lewis acid sites and by reacting cumene and benzene, herewith toluene is also formed in the last case [60]. The sample 2zt-100 exhibits a higher selectivity to styrene (2.2 mol%—at 300 °C), compared with H-ZSM-5-170 (1.5 mol%), because 2zt-100 possesses a higher concentration of Lewis acid sites (40 μmol/g, for H-ZSM-5-170—23 μmol/g), which are catalytically active in the styrene formation [61]. The reduction of selectivity to styrene by increasing the temperature of cracking up to 400 °C (to 1.3 mol% for 2zt-100, to 0.8 mol% for H-ZSM-5-170) is probably due to the fact that reaction of ethylbenzene formation occurs predominantly on Lewis acid sites in these conditions [60].

4 Conclusions

The results of conducted research show that zeolite ZSM-5 with a high degree of crystallinity comparable to that of zeolites obtained at an increased temperature (170 °C) and in alkaline media can be formed at a relatively low temperature (100 °C) in alkali-free media. It is facilitated by the high structure-directing activity and specificity of templating action of tetrapropylammonium TPA^+ cations, as well as a high concentration of reactants in the initial reaction mixtures [$H_2O/(SiO_2 + Al_2O_3) = 11$].

The differences in structural and sorption properties of zeolite ZSM-5 obtained at 100 °C, compared with isostructural analog, synthesized at 170 °C in an alkaline reaction medium—higher values of micropore and mesopore volumes, total specific surface area, less uniform micropore size distribution for ZSM-5, are caused by differences in media of zeolite formation, as well as the features of action of templates—only TPA^+ cations—in the first case, and TPA^+ and Na^+ cations—in the other.

Zeolite obtained at 100 °C has lower concentration of acid sites and broader distribution of them by strength, in comparison with zeolite synthesized at 170 °C in an alkaline medium and preferably containing Brønsted acid sites. ZSM-5 obtained at 100 °C exhibits a high catalytic activity in the reaction of cracking of cumene, as well as a higher selectivity to propylene and styrene, in comparison with isostructural analogue obtained at 170 °C in an alkaline medium.

Results of the research suggest the possibility of use the sol-precursors of ZSM-5 containing the elements of secondary building units of zeolite as the initial building material for realization of the process of dual template synthesis of micro-mesoporous aluminosilicates, that combine in some extent the properties of zeolites and mesoporous molecular sieves.

Acknowledgments The authors express their gratitude to Yulia Voloshyna and Maria Krylova from Institute of Bioorganic Chemistry and Petrochemistry of National Academy of Sciences of Ukraine for the carrying out the test reaction of catalytic cracking of cumene.

References

1. A.A. Costa, W.B. Wilson, H. Wang, A.D. Campiglia, J.A. Dias, S.C.L. Dias, Microporous Mesoporous Mater. **149**, 186 (2012)
2. J.-X. Qin, Z.-M. Wang, X.-Q. Liu, Y.-X. Li, L.-B. Sun, J. Mater. Chem. A **3**, 12247 (2015)
3. S. Zeng, S. Ding, S. Li, R. Wang, Z. Zhang, Inorg. Chem. Commun. **47**, 63 (2014)
4. M. Ben Abda, O. Schäf, Y. Zerega, Microporous Mesoporous Mater. **217**, 178 (2015)
5. U. Olsbye, S. Svelle, M. Bjørgen, P. Beato, T.V.W. Janssens, F. Joensen, S. Bordiga, K.P. Lillerud, Angew. Chemie Int. Ed. **51**, 5810 (2012)
6. S. Teketel, L.F. Lundegaard, W. Skistad, S.M. Chavan, U. Olsbye, K.P. Lillerud, P. Beato, S. Svelle, J. Catal. **327**, 22 (2015)
7. A.A. Al-Shammari, S.A. Ali, N. Al-Yassir, A.M. Aitani, K.E. Ogunronbi, K.A. Al-Majnouni, S.S. Al-Khattaf, Fuel Process. Technol. **122**, 12 (2014)
8. X. Mu, D. Wang, Y. Wang, M. Lin, S. Cheng, X. Shu, Chin. J. Catal. **34**, 69 (2013)
9. C.S. Cundy, P.A. Cox, Microporous Mesoporous Mater. **82**, 1 (2005)
10. K. Möller, T. Bein, Chem. Soc. Rev. **42**, 3689 (2013)
11. R. Chal, C. Gérardin, M. Bulut, S. van Donk, ChemCatChem **3**, 67 (2011)
12. L. Ayele, J. Pérez-Pariente, Y. Chebude, I. Díaz, Microporous Mesoporous Mater. **215**, 29 (2015)
13. S. Mintova, N.H. Olson, V. Valtchev, T. Bein, Science **283**, 958 (1999)
14. X. Zhang, D. Tang, G. Jiang, Adv. Powder Technol. **24**, 689 (2013)
15. G. Garcia, E. Cardenas, S. Cabrera, J. Hedlund, J. Mouzon, Microporous Mesoporous Mater. **219**, 29 (2016)
16. L. Tosheva, V.P. Valtchev, Chem. Mater. **17**, 2494 (2005)
17. S.F. Mousavi, M. Jafari, M. Kazemimoghadam, T. Mohammadi, Ceram. Int. **39**, 7149 (2013)
18. C.A. Fyfe, R.J. Darton, H. Mowatt, Z.S. Lin, Microporous Mesoporous Mater. **144**, 57 (2011)
19. C.S. Cundy, M.S. Henty, R.J. Plaisted, Zeolites **15**, 353 (1995)
20. C.S. Cundy, M.S. Henty, R.J. Plaisted, Zeolites **15**, 400 (1995)
21. W.J. Kim, M.C. Lee, D.T. Hayhurst, Microporous Mesoporous Mater. **26**, 133 (1998)
22. H.-S. Oh, K.-K. Kang, M.-H. Kim, H.-K. Rhee, Korean J. Chem. Eng. **18**, 113 (2001)
23. C.A. Fyfe, Z.S. Lin, C. Tong, R.J. Darton, Microporous Mesoporous Mater. **150**, 7 (2012)
24. J. Aguado, D.P. Serrano, J.M. Escola, J.M. Rodríguez, Microporous Mesoporous Mater. **75**, 41 (2004)
25. S. Hosseini, M. Taghizadeh, A. Eliassi, J. Nat. Gas Chem. **21**, 344 (2012)
26. Q. Huang, H. Vinh-Thang, A. Malekian, M. Eić, D. Trong-On, S. Kaliaguine, Microporous Mesoporous Mater. **87**, 224 (2006)
27. H. Jin, M. Bismillah Ansari, S.-E. Park, Chem. Commun. **47**, 7482 (2011)
28. G. Laugel, X. Nitsch, F. Ocampo, B. Louis, Appl. Catal. A Gen. **402**, 139 (2011)
29. C. Hammond, *The Basics of Crystallography and Diffraction*, 3rd edn. (Oxford University Press Inc., New York, 2009), pp. 216–219
30. S.G. Gregg, K.S.W. Sing, *Adsorption, Surface Area and Porosity*, 2nd edn. (Academic Press, New York, 1982), p. 94
31. A. Saito, H.C. Foley, AIChE J. **37**, 429 (1991)
32. L.-B. Sun, J.-R. Li, W. Lu, Z.-Y. Gu, Z. Luo, H.-C. Zhou, J. Am. Chem. Soc. **134**, 15923 (2012)
33. X.-Y. Liu, L.-B. Sun, X.-D. Liu, A.-G. Li, F. Lu, X.-Q. Liu, ACS Appl. Mater. Interfaces **5**, 9823 (2013)
34. E.P. Barrett, L.G. Joyner, P.P. Halenda, J. Am. Chem. Soc. **73**, 373 (1951)
35. P. Hudec, A. Smiešková, Z. Židek, P. Schneider, O. Ŝolcová, Stud. Surf. Sci. Catal. **142**, 1587 (2002)
36. M.M. Dubinin, Russ. J. Phys. Chem. **39**, 697 (1965)
37. D.P. Serrano, R.A. García, D. Otero, Appl. Catal. A Gen. **359**, 69 (2009)
38. K. Kim, R. Ryoo, H.-D. Jang, M. Choi, J. Catal. **288**, 115 (2012)
39. C.A. Emeis, J. Catal. **141**, 347 (1993)
40. K. Góra-Marek, K. Tarach, M. Choi, J. Phys. Chem. C **118**, 12266 (2014)
41. C. Jo, R. Ryoo, N. Zilkova, D. Vitvarova, J. Cejka, Catal. Sci. Technol. **3**, 2119 (2013)
42. C.E.A. Kirschhock, R. Ravishankar, F. Verspeurt, P.J. Grobet, P.A. Jacobs, J.A. Martens, J. Phys. Chem. B **103**, 4965 (1999)
43. M. Abrishamkar, A. Izadi, Microporous Mesoporous Mater. **180**, 56 (2013)
44. B.J. Schoeman, O. Regev, Zeolites **17**, 447 (1996)
45. T.A.M. Twomey, M. Mackay, H.P.C.E. Kuipers, R.W. Thompson, Zeolites **14**, 162 (1994)
46. R.M. Barrer, *Hydrothermal Chemistry of Zeolites,* Russian Transl. (Mir Publishers, Moscow, 1985), pp. 188–194, 180–183
47. M.Y. Kustova, S.B. Rasmussen, A.L. Kustov, C.H. Christensen, Appl. Catal. B Environ. **67**, 60 (2006)
48. B.J. Schoeman, J. Sterte, KONA **15**, 150 (1997)
49. R.A. García-Muñoz, D.P. Serrano, G. Vicente, M. Linares, D. Vitvarova, J. Čejka, Catal. Today **243**, 141 (2015)
50. J. Weitkamp, M. Hunger, Studies in Surface Science and Catalysis, *in Introduction to Zeolite Science and Practice*, vol. 168, 3rd edn., revised edn., ed. by J. Čejka, H. van Bekkum, A. Corma, F. Schüth (Elsevier, Amsterdam, 2007), pp. 787–835
51. J.A. Lercher, A. Jentys, Studies in Surface Science and Catalysis, *in Introduction to Zeolite Science and Practice*, vol. 168, 3rd edn., revised edn., ed. by J. Čejka, H. van Bekkum, A. Corma, F. Schüth (Elsevier, Amsterdam, 2007), pp. 435–476
52. T. Odedairo, R.J. Balasamy, S. Al-Khattaf, J. Mol. Catal. A: Chem. **345**, 21 (2011)
53. J.M. Chezeau, L. Delmotte, J.L. Guth, Z. Gabelica, Zeolites **11**, 598 (1991)
54. B.J. Schoeman, J. Sterte, J.-E. Otterstedt, Zeolites **14**, 568 (1994)
55. C.S. Tsay, A.S.T. Chiang, Microporous Mesoporous Mater. **26**, 89 (1998)
56. Q. Li, B. Mihailova, D. Creaser, J. Sterte, Microporous Mesoporous Mater. **40**, 53 (2000)
57. A. Petushkov, S. Yoon, S.C. Larsen, Microporous Mesoporous Mater. **137**, 92 (2011)
58. L. Qinghua, W. Jingwei, Y. Hao, X. Lili, W. Lijun, A. Navrotsky, Prog. Chem. **18**, 680 (2006)
59. Z. Qin, B. Shen, X. Gao, F. Lin, B. Wang, C. Xu, J. Catal. **278**, 266 (2011)
60. A. Corma, B.W. Wojciechowski, Catal. Rev. Sci. Eng. **24**, 1 (1982)
61. D. Best, B.W. Wojciechowski, J. Catal. **47**, 11 (1977)